

NJC

New Journal of Chemistry

Accepted Manuscript

A journal for new directions in chemistry

This article can be cited before page numbers have been issued, to do this please use: W. Zhang, X. Lin, F. Li, Z. Huang, C. Gong and Q. Tang, *New J. Chem.*, 2020, DOI: 10.1039/D0NJ03666H.



This is an Accepted Manuscript, which has been through the Royal Society of Chemistry peer review process and has been accepted for publication.

Accepted Manuscripts are published online shortly after acceptance, before technical editing, formatting and proof reading. Using this free service, authors can make their results available to the community, in citable form, before we publish the edited article. We will replace this Accepted Manuscript with the edited and formatted Advance Article as soon as it is available.

You can find more information about Accepted Manuscripts in the [Information for Authors](#).

Please note that technical editing may introduce minor changes to the text and/or graphics, which may alter content. The journal's standard [Terms & Conditions](#) and the [Ethical guidelines](#) still apply. In no event shall the Royal Society of Chemistry be held responsible for any errors or omissions in this Accepted Manuscript or any consequences arising from the use of any information it contains.

ARTICLE

Multicolored electrochromic and electrofluorochromic materials containing triphenylamine and benzoates

Wei-jing Zhang, Xin-cen Lin, Feng Li, Zhen-jie Huang, Cheng-bin Gong,* and Qian Tang*

Received 00th January 20xx,
Accepted 00th January 20xx

DOI: 10.1039/x0xx00000x

Six novel electrochromic materials, 4,4',4''-nitritotribenzoates (NTBAs, a–f), with donor-acceptor structure, were designed by combining cathodically electrochromic benzoates as a color-tuning unit and anodically electrochromic triphenylamine as a fluorescence-quenching unit to achieve multi-electrochromism and electrofluorochromism. The stereochemistry of the NTBAs was investigated by single-crystal X-ray diffraction. The NTBAs showed a strong blue emission in N,N-dimethylformamide. When the NTBAs were introduced into electrochromic devices (ECDs), all six ECDs showed multicolored electrochromism. All six ECDs displayed electrofluorochromic behavior, which was possibly caused by the monocationic radical formed from the oxidation of the triphenylamine center. The ester substituents markedly influenced the colored states, switching cyclability, coloration efficiency, and electrofluorochromic properties. The compounds with saturated alkyl substituents (a–c) showed three colored states, namely yellow (at ± 2.8 V), light red (at ± 3.0 V), and orange red (at ± 3.6 V), relatively better cyclability, high coloration efficiency (> 220 cm²/C), and good electrofluorochromic properties. The compound with the shortest chain length (a) performed best. The compound with an unsaturated alkyl substituent (d) showed poor electrochromic and electrofluorochromic properties. The compounds with aryl substituents (e and f) showed three colored states, namely yellow (at ± 2.6 V), purple (at ± 3.0 V), and claret (at ± 3.6 V), moderate coloration efficiency (ca. 200 cm²/C), and good electrofluorochromic properties. The cyclability was markedly improved when the aryl substituents contained an electron-donating group.

1. Introduction

Electrochromism refers to a reversible change in optical absorption during chemical reduction and oxidation.¹ Electrochromic materials (ECMs) are widely used in smart windows,^{2–5} displays,^{6–8} adaptive camouflage,^{9,10} and energy storage.^{11–13} Since Platt¹⁴ discovered the electrochromic phenomenon in 1961, a number of ECMs, including inorganic transition metal oxides,^{15–18} organic materials,^{19–22} and organic and inorganic hybrid materials,^{23–25} have been developed. Multicolored ECMs, which allow multicolor tunability, have attracted considerable research attention for their potential applications in displays such as smart windows, electronic papers, antiglare rearview mirrors, and adaptive camouflage.^{1,9} Although significant achievements have been made, the need persists for development of more easily synthesized multicolored ECMs with good multicolor tunability.

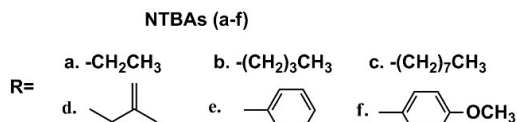
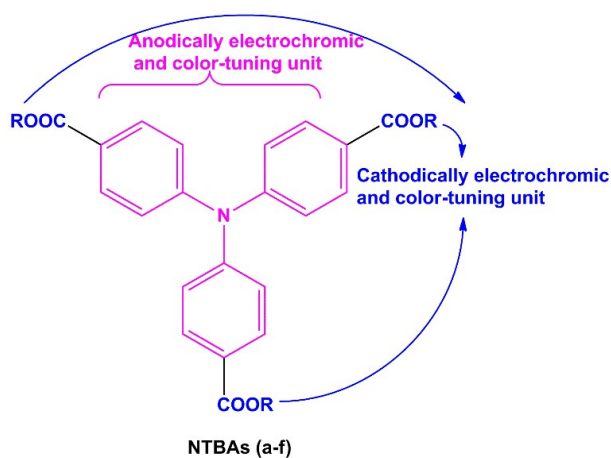
In 1993, Lehn²⁶ proposed the concept of electrofluorochromic (EFC) behavior, which combines

electrochromism and fluorescence in one material. In 2006, Kim²⁷ reported the first EFC device (EFC) based on a tetrazine containing material. EFCs have the advantages of low working voltage regime, low power requirement, and full visible-spectrum coverage, and therefore have potential application in displays, optical memory, sensors, and biological analysis.²⁸ Since 2006, many ECMs with EFC behavior,²⁹ such as materials containing boradiazaindacene,³⁰ viologens,³¹ boron dipyrromethene–ferrocene,³² conjugated polymers containing quantum dots³³ and propylenedioxythiophene–phenylene,³⁴ spirocyclic Meisenheimer complexes,³⁵ crosslinked polymers containing tetraaniline and fluorine,³⁶ thiophene-containing materials,^{37,38} and especially materials containing triphenylamine (TPA) and derivatives,^{28,39–48} have been developed. TPA and derivatives have been the most extensively studied because they are effective fluorescence quenchers through the formation of radical cations via electrochemical oxidation.⁴⁸ High-performance EFC devices, especially with multielectrochromism, are still lacking and their preparation remains a challenge.

In 1987, Sugimoto⁴⁹ discovered that phthalate derivatives showed cathodically electrochromic behavior, which laid the foundation for studying the electrochemical properties of benzoates. Webster^{50–53} studied the mechanism for the electrochemical reduction of disubstituted aromatic esters and thioic S-esters in detail. Kobayashi,⁵⁴ Webster,⁵⁵ and Gong^{56–58} reported the electrochromic properties of benzoates with different molecular structures. However, these benzoates

The Key Laboratory of Applied Chemistry of Chongqing Municipality, Chongqing Key Laboratory of Soft-Matter Material Chemistry and Function Manufacturing, College of Chemistry and Chemical Engineering, Southwest University, Chongqing, 400715, China. gongcbtq@swu.edu.cn; qiantang@swu.edu.cn

*Electronic Supplementary Information (ESI) available: [details of Synthesis and characterization of NTBAs, crystal data and structure refinement, cyclic voltammetry, electrochromic behavior, electrofluorochromic behavior, DFT calculations, and measurement of fluorescence quantum yields]. See DOI: 10.1039/x0xx00000x



Scheme 1 Molecular structure of NTBAs.

displayed only one colored state. Gong reported dual-colored electrochromic benzoates through molecular design.^{59,60} In this paper, we report novel ECMs, 4,4',4''-nitrotribenzoates (NTBAs), with D-A (donor-acceptor) structure, by combining cathodically electrochromic benzoates as a color-tuning unit and anodically electrochromic TPA as a fluorescence-quenching and color-tuning unit in one material (Scheme 1), which show both multicolored electrochromism and EFC behavior.

2. Experimental

2.1. Materials and instruments

4-Aminobenzonitrile (AR, 98%), 4-fluorobenzonitrile (AR, 99%), cesium fluoride (AR, 99%), alcohols, and phenols were purchased from Aladdin Co., Shanghai, China. Potassium hydroxide (AR, $\geq 99\%$), thionyl chloride (AR, 99%), and triethylamine (AR, 99%) were purchased from Chemical Co., Chongqing, China. The fluorescence quantum yields of solid-state molecules were measured with a FS5 fluorescence spectrometer (Edinburgh Instruments, England) by using a 150 W steady state xenon lamp and a calibrated integrating sphere. The fluorescence spectra were measured with a F-380 fluorescence spectrophotometer (Tianjin, China). The CIE (International Commission on Illumination) $L^*a^*b^*$ coordinates for the ECDs based on NTBAs was measured with a color reader CR-10 plus (Konica Minolta, Inc., Japan).

2.2. Synthesis of NTBAs

NTBAs (a-f) were synthesized according to previous methods.⁵⁶⁻⁵⁹ Details of the synthesis and characterization of all these compounds are supplied in the Supporting Information.

2.3. Fabrication of electrochromic devices

Fabrication, sealing, and testing of all ECDs were performed at room temperature according to previous methods by sandwiching the electrochromic layer between two electrodes of glass coated with indium tin oxide (conductive side inward)

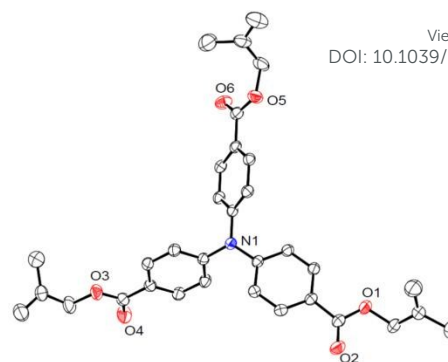


Fig. 1. ORTEP representation of compound d. Displacement ellipsoids are set to 30% probability. Hydrogen atoms are omitted for clarity.

and reflective metallic surface with a separation of 0.035 mm.^{22,56,57,59} The dimension of ECD was 20 mm in width and 20 mm in length. For the electrochromic layer, the concentrations of a-f, ferrocene, and tetrabutylammonium hexafluorophosphate (TBAPF₆) in N,N-dimethylformamide (DMF) were all 20 mmol/L.

2.4. X-ray crystal structure

Single-crystal X-ray diffraction was carried out on an Agilent SuperNova EosS2 diffractometer using graphite monochromated Cu K α radiation ($\lambda = 1.54184 \text{ \AA}$). The crystals were kept at 291.5 (10) K during data collection. The structure was solved by the ShelXT^{61,62} structure solution program in Olex2⁶³ and refined using full-matrix least squares based on F2 with the program SHELXL-2018^{61,62} within Olex2.

3. Results and discussion

3.1. Stereochemistry

A single crystal of compound d was cultured at room temperature in a mixed solvent of dichloromethane and ethanol with a volume ratio of 2:1. Fig. 1 depicts the X-ray crystal structure of compound d. Crystal data and experimental data for compound d are summarized in Table S1 (see Supporting Information).

3.2. Density functional theory calculations

To further understand the electrochemical and electrochromic mechanism, representative compounds a, d, and f were selected for density functional theory (DFT) calculations. The calculations were performed by using the Gaussian 09 program package. All the geometries of compounds were fully optimized by using the Becke three-parameter hybrid functional (B3LYP) at 6-31g* basis set. The solvent effects of DMF were simulated by using a polarizable continuum model PCM with the self-consistent reaction field SCRF method. The UV-Vis spectra were simulated under the same condition with TDDFT PBE0/6-31g* method. The energy levels were listed in Table S3, the simulated absorption spectra were illustrated in Fig. S25, and the molecular orbital diagrams were illustrated in Fig. 2. The HOMOs of compounds a, d, and f were predominantly found at

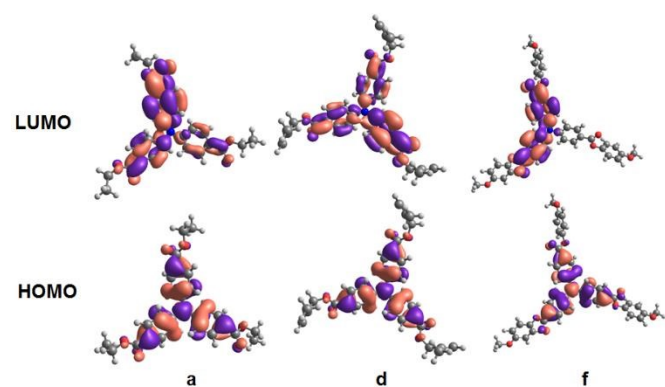


Fig. 2. The HOMO and LUMO diagram of compounds a, d, and f.

the central part of the molecules, which indicated that the central triphenylamine unit was oxidized prior to the three branched ester units.¹⁹ The LUMOs of compounds a and d were similar, the charge localized on three branches. This demonstrates that all three branches have the tendency to accept electrons. The charge at the LUMO of compound f was localized across two of the three branches, which was distinctly different from those of compounds a and d. This indicates that two branches of compound f have the tendency to accept electrons. The energy gaps of compounds a, d, and f were calculated to be 3.941, 3.934, and 3.885 eV, respectively (Table S3).

3.3. Electrochemical properties

Cyclic voltammetry (CV) of compounds a–f (1 mmol/L) was measured under a nitrogen atmosphere in DMF at room temperature using TBAPF₆ (50 mmol/L) as the supporting electrolyte (Fig. 3). The anodic peak potential (E_{pa}) and cathodic peak potential (E_{pc}) values of a–f are listed in Table 1. By combining the CV results of DMF and DMF/TBAPF₆ (Fig. S10C), we concluded that the quasi-reversible (1'/1) at about 1.60/1.45 V vs Ag/AgCl for all compounds was derived from the oxidation of the triphenylamine center to form a monocationic radical via a one-electron process.⁴⁰ The anodic peak (5') at about 1.00 V vs Ag/AgCl was ascribed to the oxidation of TBAPF₆ (Fig. S10C). Compared to viologens and viologen analogues where pyridinium is the electrochromic center,³¹ the reduction process of ester-based ECMs is more complex because of some accompanied chemical processes.⁶⁰ When R was alkyl (compounds a–d), three redox couples (2'/2, 3'/3, and 4'/4) were observed. The intensity at 2 was weak and gradually increased as the scan number increased (Fig. S9), this was possibly assigned to an adsorbed species. The peak current magnitude of 3 was much larger than that of 4, this indicated that electrochemical processes of 3'/3 and 4'/4 may have different electron transfer number. The redox couples of 3'/3 and 4'/4 probably corresponded to the reduction of the benzoate unit (Fig. 3).⁵³ To investigate the mutual interaction between the anodically (triphenylamine) and cathodically (esters) electrochromic units, CV scans were conducted at the potential between 0.0 and 2.0 V vs Ag/AgCl (Fig. S10A, S11A, S12A, and S13A) and between 0.0 to –2.6 V vs Ag/AgCl (Fig. S10B,

Table 1 The E_{pa} and E_{pc} values of compounds a–f

View Article Online

DOI: 10.1039/D0NJ05066H

Compound	E_{pa}/V vs Ag/AgCl	E_{pc}/V vs Ag/AgCl
a	1.58, –1.53, –1.81, –2.54	1.46, –1.67, –2.07, –2.70
b	1.56, –1.54, –1.8, –2.54	1.44, –1.70, –2.07, –2.68
c	1.59, –1.54, –1.82, –2.46	1.44, –1.63, –2.04, –2.58
d	1.59, –1.51, –1.79, –2.57	1.46, –1.61, –2.04, –2.69
e	1.72, –1.41, –1.59, –2.27	1.54, –1.94, –1.94, –2.44
f	1.62, –1.41, –1.63, –2.41	1.51, –1.94, –1.94, –2.54

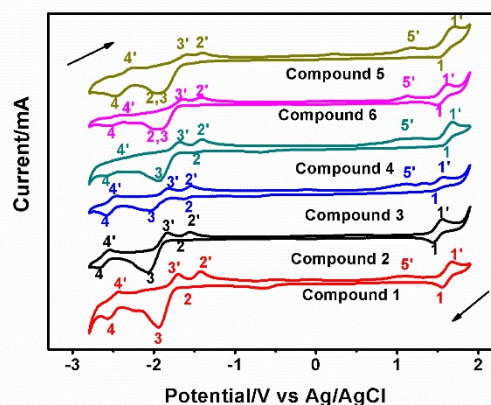


Fig. 3. CV analysis of compounds a–f (1.0 mmol/L) in DMF/TBAPF₆ (50 mmol/L) vs Ag/AgCl at room temperature and a scan rate of 300 mV s⁻¹.

S11B, S12B, and S13B). Compared with CV scans at the potential between –2.6 to 2.0 V vs Ag/AgCl, the intensity at 1 became weak, and all three redox couples (2'/2, 3'/3, and 4'/4) showed better reversibility (Fig. 3). This results indicate that the combination of esters with triphenylamine center modified their electronic properties. When R was aryl (compounds e and f, Fig. 3), three anodic peaks at 2', 3', and 4' were also observed, similar to compounds a–d, but only two cathodic peaks at ca. –1.94 and –2.54 V vs Ag/AgCl were observed. Similarly, the peak at ca. –1.94 V was broader and more intense (Fig. S9). The reductive peaks of 3 and 4 were also attributed to the reduction of the benzoate unit. CV scans were also conducted at the potential between 0.0 and 2.0 V vs Ag/AgCl for e and f (Fig. S14A and S15A), and between 0.0 to –2.4 V vs Ag/AgCl vs Ag/AgCl for e (Fig. S14B) and between 0.0 to –2.5 V vs Ag/AgCl for f (Fig. S15B). Compared with CV scans at the potential between –2.5 (–2.4) to 2.0 V vs Ag/AgCl, the intensity at 1 and 4' became weak, and a cathodic peak at 2 with weak intensity appeared. This results also demonstrates that the combination of esters with triphenylamine center modified their electronic properties.

3.4. Electrochromic properties

The UV-Vis spectra of the ECDs based on compounds a–f were measured in air to demonstrate the electrochromic characteristics of these materials (Fig. 4, Fig. S16, and Fig. S17 in Supporting Information).⁴⁵ In the absence of an applied voltage,

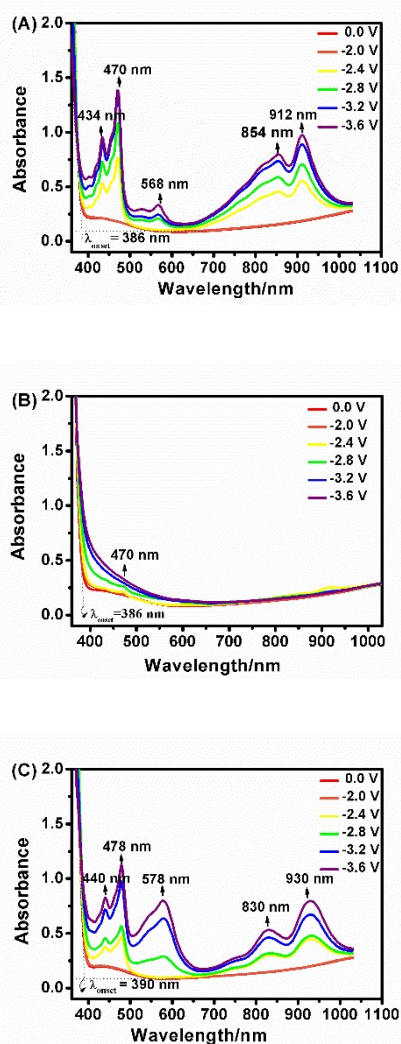


Fig. 4. UV-Vis spectra of ECDs based on compound a (A), d (B), and f (C) with a concentration of 20 mmol/L on indium tin oxide-coated glass at different potentials from -2.0 to -3.6 V.

all compounds were in a neutral state, and a weak and broad absorption peak at around 456 nm was observed, which was ascribed to the intramolecular $\pi-\pi^*$ transition. All ECDs based on compounds a–f displayed a bleached transparent state (Fig. 5 and Fig. S18 in Supporting Information). When R was a saturated alkyl group (compounds a–c), new absorption peaks at about 434, 470, 568, 854, and 912 nm appeared, accompanied by the disappearance of the absorption at ca. 456 nm when the applied voltage reached ± 2.4 V due to electrochemical process. The absorption intensity increased as the applied voltage further increased and reached saturation at ± 3.2 V. When R was an alkyl group containing an unsaturated C=C bond (compound d), only a very weak absorption peak at 470 nm was observed at applied voltages $< \pm 3.0$ V, and the absorption peak completely disappeared when the applied



Fig. 5. Photograph of the ECDs based on compounds a (A) and f (B) in their bleached (at 0.0 V) and colored states.

voltage was further increased, probably because of material aging (Fig. 4B). When R was benzyl (compounds e and f), new absorption peaks at about 440, 478, 578, 830, and 930 nm appeared, which were slightly red-shifted compared with compounds a–c because of the greater degree of conjugation. All ECDs based on compounds a–f displayed multicolored states (Fig. 5 and Fig. S18 in Supporting Information). The first colored state was yellow at ± 2.8 V for compounds a–d and ± 2.6 V for compounds e and f, and was ascribed to the oxidation of the central triphenylamine to radical cations; the second colored state was light red for compounds a–d and purple for compounds e and f at ± 3.0 V, and was ascribed to the reduction process of 3 in Fig. 3; and the third colored state was orange red for compounds a–d and claret for compounds e and f at ± 3.6 V, and was ascribed to the reduction process of 4 in Fig. 3.⁵³ Although the ECDs based on compounds c and d exhibited different spectroelectrochemistry (Fig. S16B and Fig. 4B), they showed similar colored states (Fig. S18). This indicated that they underwent similar electrochemical processes. The difference in spectroelectrochemistry was ascribed to the poor stability of compound d. The spectroelectrochemistry in the positive potentials was measured, and the results were supplied in supporting information as Fig. S17. No distinct changes in both absorption peaks and onset voltages were observed. This was assigned to the characteristic of liquid-state ECDs, where the electrochromic materials and electrolyte were dissolved in a proper solvent, and were simply sandwiched between two electrodes of ITO-coated glasses. Thus, applying bias between two electrodes at positive or negative directions can't generate obvious difference in UV-Vis spectra. The CIE $L^*a^*b^*$ coordinates for the ECDs based on compounds a–f in the bleached and colored states are listed in Table S2.

To study the electrochromic switching properties of compounds a–f, the corresponding ECDs were switched at room temperature in air by repeated potential steps between the three oxidized states (with an applied voltages of +2.8 V for compounds a–d and +2.6 V for compounds e and f; +3.0 V and +3.6 V) and reduced states (with an applied voltages of -2.8 V for compounds a–d and -2.6 V for compounds e and f; -3.0 V and -3.6 V) with a residence time of 4 s at $\lambda_{max}^{22,45,56-59,64}$. The optical contrast ($\Delta T\%$) is defined as the change in transmittance between the reduced and oxidized states.⁵⁶ Fig. 6 and Fig. S19 (Supporting Information) show the optical switching changes

for the ECDs based on compounds a–f. When R was a saturated alkyl group (compounds a–c), at the first colored state with an applied voltage of ± 2.8 V, the maximum $\Delta T\%$ for the ECDs based on compounds a–c were 56%, 57%, and 45%, and decreased to 41%, 39%, and 28% after 2000 s; at the second colored state with an applied voltage of ± 3.0 V, the maximum $\Delta T\%$ for the ECDs based on compounds a–c were 60%, 46%, and 55%, and fell to 58%, 40%, and 35% after 2000 s; at the third colored state with an applied voltage of ± 3.6 V, the maximum $\Delta T\%$ for the ECDs based on compounds a–c were 67%, 56%, and 99%, and decreased to 35%, 10%, and 26% after 2000 s for compound a and 1000 s for compounds b and c. The second of the three colored states showed the best switching stability. This was ascribed to the donor-acceptor structure which allows intermolecular charge transfer. When R was an alkyl group containing an unsaturated C=C bond (compound d), the maximum $\Delta T\%$ was low and the cyclability at both the first and the second colored states was poor (Fig. S19G and H in Supporting Information), which was consistent with the UV-Vis spectra. As plausible reason for this result cannot be derived from DFT calculation and CV results, the electrochromic properties of three compounds, tris(4-(trifluoromethyl)phenyl) 4,4',4''-nitrotribenzoate, tribenzyl 4,4',4''-nitrotribenzoate, and tris(4-methoxybenzyl) 4,4',4''-nitrotribenzoate, were investigated (Fig. S20). Tris(4-(trifluoromethyl)phenyl) 4,4',4''-nitrotribenzoate and tribenzyl 4,4',4''-nitrotribenzoate showed poor electrochromic properties, which was similar to compound d. Compared with tribenzyl 4,4',4''-nitrotribenzoate,

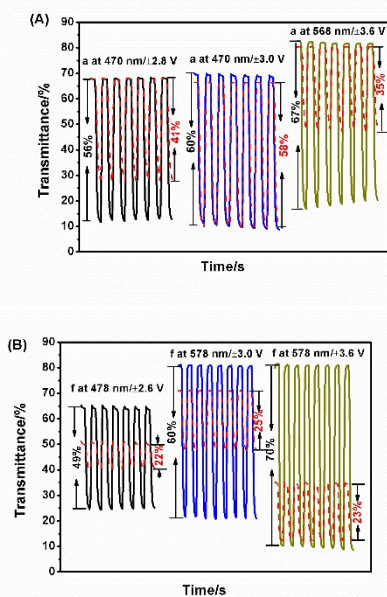


Fig. 6. Optical switching behavior of electrochromic devices at 470 nm as a function of time between -2.8 V and 2.8 V and -3.0 V and 3.0 V, and at 568 nm as a function of time between -3.6 V and 3.6 V for compound a (A), and at 478 nm as a function of time between -2.6 V and 2.6 V, and at 578 nm as a function of time between -3.0 V and 3.0 V and -3.6 V and 3.6 V for compound f with a residence time of 4 s (B). The red dashed lines represent their corresponding optical switching after 2000 s.

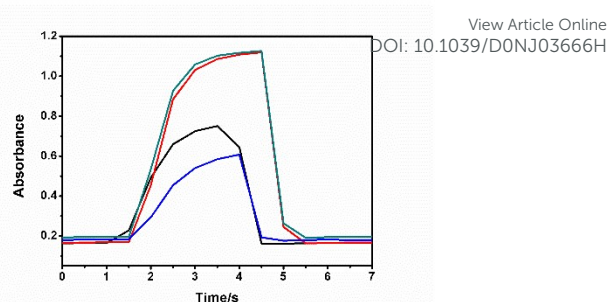


Fig. 7. Electrochromic switching responses of electrochromic devices at 470 nm as a function of time between -2.8 V and 2.8 V (black curve) and -3.0 V and 3.0 V (blue curve) for a, and at 478 nm as a function of time between -2.6 V and 2.6 V (blue curve) and -3.0 V and 3.0 V (dark cyan) for f with a residence time of 4 s.

Table 2 Switching time and coloration efficiency data for ECDs based on compounds a–f

Compounds	Response Time/s		CE (cm^2/C)	
	t_c/t_b at ± 2.8 V	t_c/t_b at ± 3.0 V	± 2.8 V	± 3.0 V
a	1.90/0.99	1.98/0.96	256	298
b	1.96/0.96	1.84/0.69	223	270
c	1.90/1.48	1.66/0.58	233	278
d	1.77/0.47	2.47/0.87	31	46
e	1.52/0.47	1.73/0.82	186	211
f	2.04/0.49	1.74/0.63	203	188

tris(4-methoxybenzyl) 4,4',4''-nitrotribenzoate (which has an electron-donating group $-\text{OCH}_3$) showed improved electrochromic properties. This result indicates that the poor electrochromic properties of compound d and tris(4-(trifluoromethyl)phenyl) 4,4',4''-nitrotribenzoate, tribenzyl 4,4',4''-nitrotribenzoate was possibly ascribed to the electron-withdrawing characteristics of C=C bond, trifluoromethyl, and benzene.

When R was phenyl (compound e), the maximum $\Delta T\%$ was 44% at the first colored state with an applied voltage of ± 2.6 V and 54% at the second colored state with an applied voltage of ± 3.0 V, and the cyclability was poor: the maximum $\Delta T\%$ decreased to 19% and 8% after 800 s (Fig. S19I and J in Supporting Information). When R was phenyl with an electron-donating substituent ($-\text{OCH}_3$) (compound f), the cyclability was markedly improved compared with compound e. The maximum $\Delta T\%$ was 49% at the first colored state with an applied voltage of ± 2.6 V, 60% at the second colored state with an applied voltage of ± 3.0 V, and 70% at the third colored state with an applied voltage of ± 3.6 V, and fell to 22%, 25%, and 23% after 2000 s. A possible reason for the better cyclability of the ECD based on f is that the ester group attached to the benzene ring had more electron density because of the strong electron-donating effect of the methoxy group.⁵⁸

The response time is the time required to indicate the color change of an ECM between the reduced and oxidized states,⁵⁹ and is usually expressed as 95% of the total absorbance span for the coloring process (t_c) and bleaching process (t_b).⁵⁹ As shown

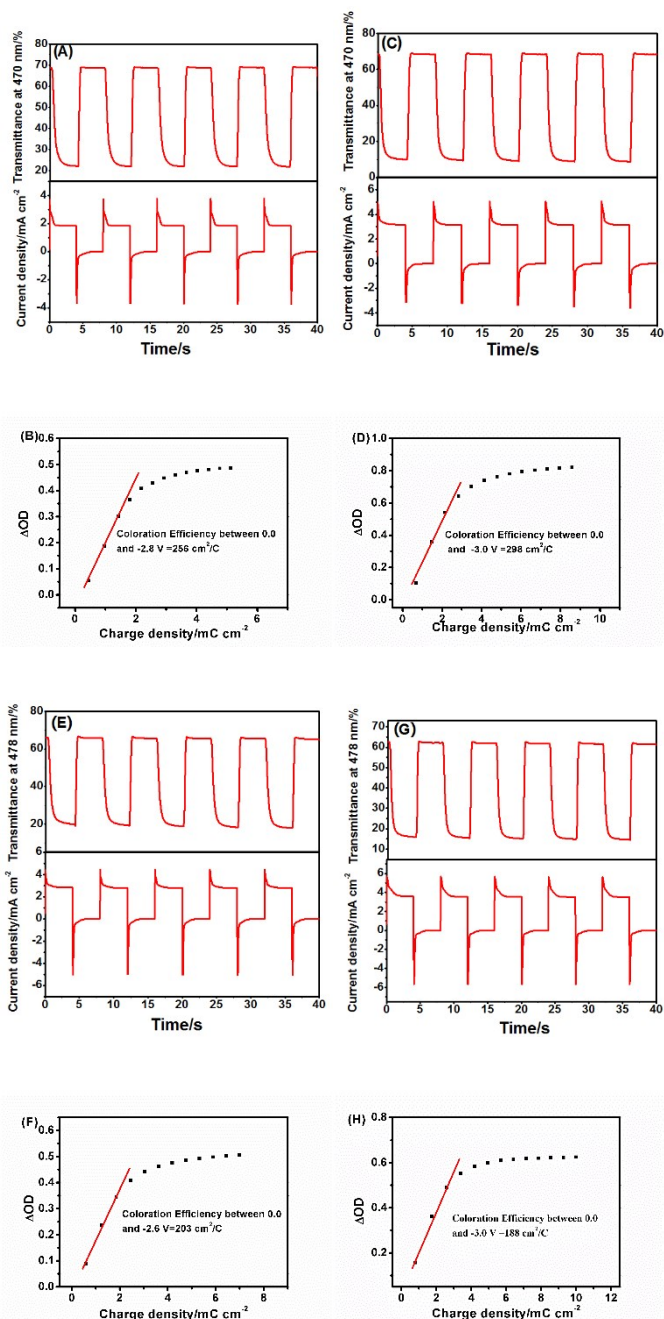


Fig. 8. Chronoamperometry curves and the corresponding in-situ transmittance curves between 0.0 and -2.8 V (A) and 0.0 and -3.0 V (C), and optical density vs charge density between 0.0 and -2.8 V (B) and 0.0 and -3.0 V (D) of the ECD based on compound a. Chronoamperometry curves and the corresponding in-situ transmittance curves between 0.0 and -2.6 V (E) and 0.0 and -3.0 V (G), and optical density vs charge density between 0.0 and -2.6 V (F) and 0.0 and -3.0 V (H) of the ECD based on compound f.

in Fig. 7, Fig. S21, and Table 2, the ECDs based on compounds a–f had a switching time of ca. 2 s for coloring and <1 s for bleaching. The difference in coloring and bleaching time was ascribed to the difference between the time constants for ejection/insertion of ions from/to the electrochromic layer.⁶⁵

The coloration efficiency (CE) represents the amount of electrochromic color formed by the charge consumed, and is calculated using Eq. 1.

$$CE(\eta) = \frac{\Delta OD}{Q_d} \quad (1)$$

$$\Delta OD = \log \frac{T_b}{T_c} \quad (2)$$

where ΔOD (optical density) represents the absorbance during the doping (dedoping) process, which was calculated from the light transmittances of the bleached (T_b) and colored (T_c) states of the ECD at a certain wavelength using Eq. 2, and Q_d is the amount of injected/ejected charge per unit sample area during a redox step of the ECD.²² Fig. 8A, 8C, 8E, 8G, and S22 (in Supporting Information) show the chronoamperometry curves and the corresponding in-situ transmittance curves of the ECDs based on compounds a–f at -2.8 and -3.0 V for a–d and at -2.6 and -3.0 V for e and f. The relationship between ΔOD and Q_d was calculated from the chronoamperometry curves and the corresponding in-situ transmittance curves (Fig. 8B, 8D, 8F, 8H, and S23 in Supporting Information). The CE values of compounds a–f were estimated by fitting the slope of the linear plots of ΔOD vs Q_d according to the method reported by Xiao,⁶⁷ and the results are listed in Table 2. The ECDs based on compounds a–c (>200 cm^2/C) have higher CE values than those based on compounds e and f (ca. 200 cm^2/C). The ECD based on compound d has the lowest CE values (<50 cm^2/C) at both the first and second states.

3.5. Optical and electrofluorochromic properties

The UV-Vis spectra of a–f were investigated in DMF (20 $\mu\text{mol}/\text{L}$) at room temperature. All compounds have a similar maximum absorption wavelength centered at 348 nm for a–d, 350 nm for e, and 356 nm for f. As shown in Fig. 9A, S24A, S25 and Table S4, the absorption spectra were compatible with experimental results. The fluorescence behaviors of compounds a–f were also investigated in DMF solution (20 $\mu\text{mol}/\text{L}$) at room temperature, excited at 358 nm. All compounds showed a strong fluorescence emission spectrum at 434 nm for a, 420 nm for b, 424 nm for c, 416 nm for d, 417 nm for e, and 420 nm for f with a blue emission (Fig. 9B and S24B). The fluorescence quantum yields of compounds a–f were measured to be 14.05%, 14.22%, 32.16%, 12.75%, 23.87%, and 2.08%, respectively (Fig. S27–32 and Table S5).⁴⁵ The ECDs based on compounds a–f showed electrofluorochromic behavior. Under irradiation at 365 nm, all ECDs showed blue emission in their bleached state at an applied voltage of 0.0 V, possibly attributable to intramolecular photo-induced electron transfer, whereas the fluorescence was partially and completely quenched in the colored states at applied voltages of $+2.8$ and $+3.5$ V, respectively, for compounds a–c, e, and f (Fig. 9C and S24C). For compound d, which has poor electrochromic properties, the quenching effect was not as strong as for the other five compounds. The quenched behavior of the ECDs based on compounds a–f was ascribed to the monocationic radical formed from the oxidation of the triphenylamine center, which has been reported to be an effective quencher.⁴⁸ We also found that the quenching was

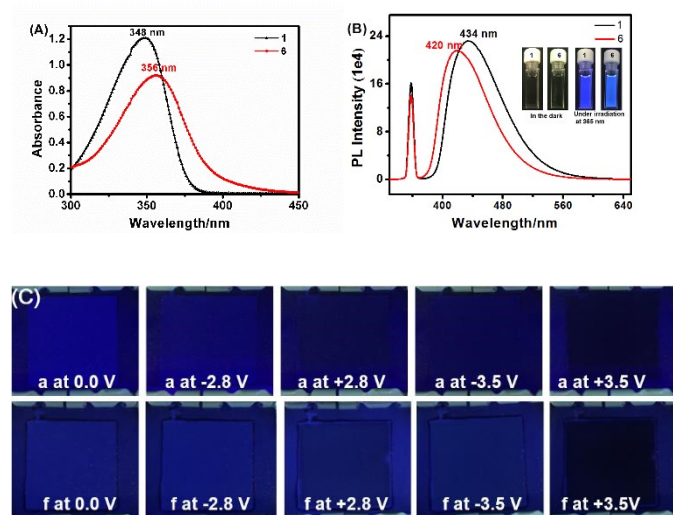


Fig. 9. UV-Vis (A) and fluorescence (B) spectra of compounds a and f (2×10^{-5} mol/L) in DMF excited at 358 nm. Photographs of the ECDs based on compounds a and f in their bleached (0.0 V) and colored states (± 2.8 and ± 3.5 V) under irradiation at 365 nm (C). The inset photographs in (B) were taken in the dark and under illumination at 365 nm.

slightly weaker at negative applied voltages (-2.8 and -3.5 V) than at positive applied voltages ($+2.8$ and $+3.5$ V) (Fig. 9C and S24C). These results show that the formation of monocationic radicals by positive applied voltages was beneficial to the EFC behavior. As inapparent changes were observed in spectroelectrochemistry by applying bias at positive or negative directions, this was possibly attributed to that fluorescent behaviour was more sensitive than UV-Vis spectra. The stability of EFC behaviour was similar to the electrochromic cycling stability of the corresponding ECM.

Tetraphenylethylene cored benzoates, 4,4',4'',4'''-(ethene-1,1,2,2-tetrayl)tetrabenzoates, displayed an aggregation-induced emission, a monocolored state of blue, an onset voltage of ca. -1.8 V, a high optical contrast of ca. 80%, coloration efficiencies of >127 cm^2/C , and a coloring time of >1.85 s and a bleaching time of >1.2 s.⁶⁸ Compared to 4,4',4'',4'''-(ethene-1,1,2,2-tetrayl)tetrabenzoates, NTBAs displayed an EFC behavior, multicolored electrochromism, an onset voltage of ca. -2.0 V, a slightly lower optical contrast of ca. 60%, a higher coloration efficiency except compound d, and a rapid response time.

Conclusions

In summary, six novel electrochromic materials (NTBAs, a–f) with D-A structure were synthesized by combining cathodically electrochromic benzoates as a color-tuning unit and anodically electrochromic TPA as a fluorescence-quenching unit in one material, and were fabricated into ECDs. The NTBAs exhibited a strong blue emission in DMF and in the ECDs. All six ECDs showed multicolored electrochromism and EFC behavior. The second colored states had the best switching cyclability. The

fluorescence-quenching effect was possibly caused by the monocationic radical formed from the oxidation of the triphenylamine center. The ester substituents markedly influenced the colored state, switching cyclability, coloration efficiency, and electrofluorochromic properties. The compounds with saturated alkyl substituents (a–c) showed three colored states, namely yellow, light red, and orange red, better cyclability, high coloration efficiency, and good electrofluorochromic properties. The compound with the shortest chain length (a) performed best. The compound with an unsaturated alkyl substituent (d) showed poor electrochromic and electrofluorochromic properties. The compounds with aryl substituents (e and f) showed three colored states, namely yellow (at -2.6 V), purple (at -3.0 V), and claret (at -3.6 V), a moderate coloration efficiency, and good electrofluorochromic properties. The cyclability was markedly improved when the aryl substituents contained an electron-donating group. This work provides a new pathway for design of emission/color dual-switchable materials, which can be applied in smart windows, displays, optoelectronics, sensors, and biological analysis. However, great improvement in cycling stability is required for practical application.

Conflicts of interest

There are no conflicts to declare.

Acknowledgements

The authors thank the financial support from Fundamental Research Funds for the Central Universities (XDJK2019AA003), Chongqing Municipal Education Commission (CY200240 and CY200241), and Chongqing Science and Technology Commission (cstc2017shmsA90014).

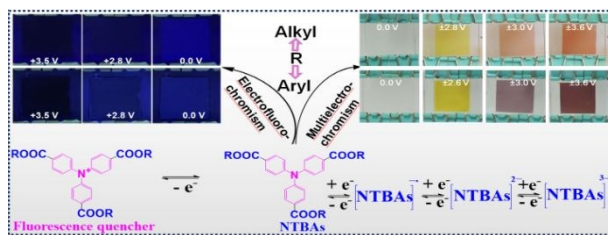
Notes and references

- Z. Liang, K. Nakamura and N. Kobayashi, *Sol. Energy Mater. Sol. Cells*, 2019, **200**, 109914.
- Z. G. Wang, M. S. Zhu, S. Y. Gou, Z. Pang, Y. Wang, Y. B. Su, Y. Huang, Q. H. Weng, O. G. Schmidt and J. Z. Xu, *ACS Appl. Mater. Interfaces*, 2018, **10**, 31697-31703.
- H. Z. Li, L. McRae, C. J. Firby, M. Al-Hussein and A. Y. Elezabi, *Nano Energy*, 2018, **47**, 130-139.
- J. R. Jennings, W. Y. Lim, S. M. Zakeeruddin, M. Gratzel and Q. Wang, *ACS Appl. Mater. Interfaces*, 2015, **7**, 2827-2832.
- A. W. Lang, Y. Y. Li, M. D. Keersmaecker, D. E. Shen, A. M. Österholm, L. Berglund and J. R. Reynolds, *ChemSusChem*, 2018, **11**, 854-863.
- J. W. Kim and J. M. Myoung, *Adv. Funct. Mater.*, 2019, **29**, 1808911.
- J. Ko, A. Surendran, B. Febriansyah and W. L. Leong, *Org. Electron.*, 2019, **71**, 199-205.
- J. Remmele, D. E. Shen, T. Mustonen and N. Fruehauf, *ACS Appl. Mater. Interfaces*, 2015, **7**, 12001-12008.
- S. Beaupre, A. C. Breton, J. Dumas and M. Leclerc, *Chem. Mater.*, 2009, **21**, 1504-1513.
- H. Yu, S. Shao, L. Yan, H. Meng, Y. He, C. Yao, P. Xu, X. Zhang, W. Hu and W. Huang, *J. Mater. Chem. C*, 2016, **4**, 2269-2273.

- 11 P. H. Yang, P. Sun, Z. S. Chai, L. H. Huang, X. Cai, S. Z. Tan, J. H. Song, W. J. Mai, *Angew. Chem. Int. Ed.*, 2014, **53**, 11935-11939.
- 12 Z. J. Bi, X. M. Li, Y. B. Chen, X. L. He, X. K. Xu and X. D. Gao, *ACS Appl. Mater. Interfaces*, 2017, **9**, 29872-29880.
- 13 Y. Zhong, Z. S. Chai, Z. M. Liang, P. Sun, W. G. Xie, C. X. Zhao and W. J. Mai, *ACS Appl. Mater. Interfaces*, 2017, **9**, 34085-34092.
- 14 J. R. Platt, *J. Chem. Phys.*, 1961, **34**, 862-863.
- 15 D. Y. Ma, T. L. Li, Z. P. Xu, L. X. Wang and J. M. Wang, *Sol. Energy Mater. Sol. Cells*, 2018, **177**, 51-56.
- 16 L. L. Zhu, C. K. N. Peh, T. Zhu, Y. F. Lim and G. W. Ho, *J. Mater. Chem. A*, 2017, **5**, 8343-8351.
- 17 H. Y. Qu, D. Primetzhofer, M. A. Arvizu, Z. Qiu, U. Cindemir, C. G. Granqvist and G. A. Niklasson, *ACS Appl. Mater. Interfaces*, 2017, **9**, 42420-42424.
- 18 R. Venkatesh, C. R. Dhas, R. Sivakumar, T. Dhandayuthapani, P. Sudhagar, C. Sanjeeviraja and A. M. E. Raj, *J. Phys. Chem. Solids*, 2018, **122**, 118-129.
- 19 G. A. Corrente, E. Fabiano, F. Manni, G. Chidichimo, G. Gigli, A. Beneduci, A. L. Capodilupo, *Chem. Mater.*, 2018, **30**, 5610-5620.
- 20 X. C. Lin, N. Li, W. J. Zhang, Z. J. Huang, Q. Tang, C. B. Gong and X. K. Fu, *Dyes Pigments*, 2019, **171**, 107783.
- 21 F. Li, Z. J. Huang, Q. H. Zhou, M. Y. Pan, Q. Tang and C. B. Gong, *J. Mater. Chem. C*, 2020, DOI: 10.1039/d0tc00250j.
- 22 K. Ma, Q. Tang, C. R. Zhu, J. F. Long, C. B. Gong and X. K. Fu, *Electrochim. Acta*, 2018, **259**, 986-993.
- 23 B. C. Pan, W. H. Chen, T. M. Lee and G. S. Liou, *J. Mater. Chem. C*, 2018, **6**, 12422-12428.
- 24 S. H. Zhang, S. Chen, F. Yang, F. Hu, B. Yan, Y. C. Gu, H. Jiang, Y. Cao and M. Xiang, *Org. Electron.*, 2019, **65**, 341-348.
- 25 J. Wang, J. F. Wang, M. Chen, D. J. Qian and M. H. Liu, *Electrochim. Acta*, 2017, **251**, 562-572.
- 26 V. Gouille, A. Harriman and J. M. Lehn, *J. Chem. Soc., Chem. Commun.*, 1993, **6**, 1034-1036.
- 27 Y. Kim, E. Kim, G. Clavier and P. Audebert, *Chem. Commun.*, 2006, **34**, 3612-3614.
- 28 M. Pietsch, T. Rodlmeier, S. Schliske, J. Zimmermann, C. Romero-Nieto and G. Hernandez-Sosa, *J. Mater. Chem. C*, 2019, **7**, 7121-7127.
- 29 P. Audebert and F. Miomandre, *Chem. Sci.*, 2013, **4**, 575-584.
- 30 N. L. Bill, J. M. Lim, C. M. Davis, S. Bahring, J. O. Jeppesen, D. Kim and J. L. Sessler, *Chem. Commun.*, 2014, **50**, 6758-6761.
- 31 Y. C. Shi, J. Liu, M. Li, J. M. Zheng and C. Y. Xu, *Electrochim. Acta*, 2018, **285**, 415-423.
- 32 O. Galangau, I. Fabre-Francke, S. Munteanu, C. Dumas-Verdes, G. Clavier, R. Méallet-Renault, R. B. Pansu, F. Hartl and F. Miomandre, *Electrochim. Acta*, 2013, **87**, 809-815.
- 33 J. Liu, G. Luo, S. Mi, J. M. Zheng and C. Y. Xu, *Sol. Energy Mater. Sol. Cells*, 2018, **177**, 82-88.
- 34 X. Yang, S. Seo, C. Park and E. Kim, *Macromolecules*, 2014, **47**, 7043-7051.
- 35 M. Villabona, M. Benet, S. Mena, R. O. Al-Kaysi, J. Hernando and G. Guirado, *J. Org. Chem.*, 2018, **83**, 9166-9177.
- 36 Y. Y. Li, Y. Zhou, X. T. Jia and D. M. Chao, *J. Electroanal. Chem.*, 2018, **823**, 672-677.
- 37 J. C. Wu, Y. F. Han, J. Liu, Y. C. Shi, J. M. Zheng and C. Y. Xu, *Org. Electron.*, 2018, **62**, 481-490.
- 38 J. Liu, M. Li, J. C. Wu, Y. C. Shi, J. M. Zheng and C. Y. Xu, *Org. Electron.*, 2017, **51**, 295-303.
- 39 Q. Y. Lu, C. Y. Yang, X. Qiao, X. Zhang, W. Cai, Y. Chen, Y. Wang, W. Zhang, X. X. Lin, H. J. Niu and W. Wang, *Dyes Pigments*, 2019, **166**, 340-349.
- 40 N. W. Sun, S. Y. Meng, Z. W. Zhou, D. M. Chao, Y. Yu, K. X. Su, D. M. Wang, X. G. Zhao, H. W. Zhou and C. H. Chen, *Electrochim. Acta*, 2017, **256**, 119-128.
- 41 N. W. Sun, K. X. Su, Z. W. Zhou, X. Z. Tian, J. H. Zhao, D. M. Chao, D. M. Wang, F. Lissel, X. G. Zhao and C. H. Chen, *Macromolecules*, 2019, **52**, 5131-5139.
- 42 N. W. Sun, K. X. Su, Z. W. Zhou, Y. Yu, X. Z. Tian, D. M. Wang, X. G. Zhao, H. W. Zhou and C. H. Chen, *ACS Appl. Mater. Interfaces*, 2018, **10**, 16105-16112.
- 43 K. X. Su, N. W. Sun, X. Z. Tian, S. Guo, Z. H. Yan, D. M. Wang, H. W. Zhou, X. G. Zhao and C. H. Chen, *J. Mater. Chem. C*, 2019, **7**, 4644-4652.
- 44 C. P. Kuo, C. N. Chuang, C. L. Chang, M. Leung, H. Y. Lian and K. C. W. Wu, *J. Mater. Chem. C*, 2013, **1**, 2121-2130.
- 45 J. T. Wu, H. T. Lin and G. S. Liou, *ACS Appl. Mater. Interfaces*, 2019, **11**, 14902-14908.
- 46 H. J. Yen and G. S. Liou, *Prog. Polym. Sci.*, 2019, **89**, 250-287.
- 47 S. Y. Chen, Y. W. Chiu and G. S. Liou, *Nanoscale*, 2019, **11**, 8597-8603.
- 48 C. P. Kuo, C. L. Chang, C. W. Hu, C. N. Chuang, K. C. Ho, M. K. Leung, *ACS Appl. Mater. Interfaces*, 2014, **6**, 17402-17409.
- 49 K. Nakamura, Y. Oda, T. Sekikawa and M. Sugimoto, *Jpn. J. Appl. Phys.*, 1987, **26**, 931-935.
- 50 R. D. Webster and A. M. Bond, *J. Chem. Soc., Perkin Trans.*, 1997, **2**, 1075-1079.
- 51 R. D. Webster, A. M. Bond and D. C. Coomber, *J. Electroanal. Chem.*, 1998, **422**, 217-227.
- 52 R. D. Webster, *J. Chem. Soc., Perkin Trans. 2*, 1999, 263-269.
- 53 R. D. Webster, *J. Chem. Soc., Perkin Trans. 2*, 2002, 1882-1888.
- 54 H. Urano, S. Sunohara, H. Ohtomo and N. Kobayashi, *J. Mater. Chem.*, 2004, **14**, 2366-2368.
- 55 X. H. Xu and R. D. Webster, *RSC Adv.*, 2014, **4**, 18100-18107.
- 56 L. H. He, G. M. Wang, Q. Tang, X. K. Fu and C. B. Gong, *J. Mater. Chem. C*, 2014, **2**, 8162-8169.
- 57 Q. Tang, L. H. He, Y. H. Yang, J. F. Long, X. K. Fu and C. B. Gong, *Org. Electron.*, 2016, **30**, 200-206.
- 58 W. J. Zhang, C. R. Zhu, Z. J. Huang, C. B. Gong, Q. Tang and X. K. Fu, *Org. Electron.*, 2019, **67**, 302-310.
- 59 J. F. Long, Q. Tang, Z. Lv, C. R. Zhu, X. K. Fu and C. B. Gong, *Electrochim. Acta*, 2017, **248**, 1-10.
- 60 C. R. Zhu, J. P. Xie, H. R. Mou, Z. J. Huang, Q. Tang, C. B. Gong and X. K. Fu, *New J. Chem.*, 2019, **43**, 13654-13661.
- 61 G. M. Sheldrick, *Acta Cryst. A*, 2015, **71**, 3-8.
- 62 G. M. Sheldrick, *Acta Cryst. C*, 2015, **71**, 3-8.
- 63 O. V. Dolomanov, L. J. Bourhis, R. J. Gildea, J. A. K. Howard and H. Puschmann, *J. Appl. Cryst.*, 2009, **42**, 339-341.
- 64 C. B. Gong, L. H. He, J. F. Long, L. T. Liu, S. Liu, Q. Tang and X. K. Fu, *Synthetic Met.*, 2016, **220**, 147-154.
- 65 G. Wang, X. K. Fu, J. Huang, C. L. Wu, L. Wu and Q. L. Du, *Org. Electron.*, 2011, **12**, 1216-1222.
- 66 P. Data, P. Zassowski, M. Lapkowski, J. V. Grazulevicius, N. A. Kukhta and R. R. Reghu, *Electrochim. Acta*, 2016, **192**, 283-295.
- 67 S. Zhao, W. D. Huang, Z. S. Guan, B. Jin and D. B. Xiao, *Electrochim. Acta*, 2019, **298**, 533-540.
- 68 Z. J. Huang, H. R. Mou, J. P. Xie, F. Li, C. B. Gong, Q. Tang and X. K. Fu, *Sol. Energy Mater. Sol. Cells*, 2020, **206**, 110293.

Downloaded on 9/20/2020 9:52:30 AM. Published on 9 September 2020. Downloaded by University of Cambridge.

Table of Contents

View Article Online
DOI: 10.1039/D0NJ03666H

Multicolored electrochromic and electrofluorochromic materials containing triphenylamine and benzoates was developed